

An extended segment pattern dictionary for pattern matching tracking algorithm at BESIII *

MA Changli¹ ZHANG Yao² YUAN Ye^{2;1)} LU Xiao-Rui^{1;2)}

ZHENG Yangheng^{1;3)} He Kangli² Li Weidong²

Liu Huaiming² MA Qiumei² Wu Linghui²

¹ Graduate University of Chinese Academy of Sciences, Beijing 100049, P. R. China

² Institute of High Energy Physics, Beijing 100049, P. R. China

Abstract: A pattern matching based tracking algorithm, named MdcPatRec, is used for the reconstruction of charged tracks in the drift chamber of the BESIII detector. This paper addresses the shortage of segment finding in MdcPatRec algorithm. An extended segment construction scheme and the corresponding pattern dictionary are presented. Evaluation with Monte-Carlo and experimental data show that the new method can achieve higher efficiency for low transverse momentum tracks.

Key words: drift chamber, track reconstruction, pattern matching, pattern dictionary

PACS: 13.25.Gv, 14.20.Pt, 14.40.Be

1 Introduction

The Beijing Electron Positron Collider II (BEPCII) [1] is a double-ring multi-bunch e^+e^- collider which is operated in the collision energy range from 2 GeV to 4.6 GeV. The Beijing Spectrometer III (BESIII) [1] is a general-purpose detector with 93% coverage of full solid angle. BEPCII and BESIII are powerful facilities for the study of charmonium physics, D-physics, hadron spectroscopy and τ physics [2]. From the interaction area of the e^+e^- beams to the outside, there are 5 apparatuses: a drift chamber (MDC) [3], which includes 43 layers of drift cells and is used for charged tracking; a time-of-flight counter, which is composed of 2 layers of scintillator bars for measuring the flight time of penetrating charged particles; an electromagnetic calorimeter, which comprises 6240 CsI(Tl) crystals for the measurement of photon energy; a super-conducting solenoid magnet, which provides a 1 Tesla magnetic field and a muon counter, which includes 1000 m² resistive plate chambers, used for identifying muon.

MDC is a carbon fiber cylinder flowed with a mixture of He and C₃H₈ (He/C₃H₈ = 60/40) as working gas, and with signal and field wires strung between the two end-

caps. The signal wires are operated with a high positive voltage, while the field wires are at ground voltage. There are 6796 signal wires in total; each of them is surrounded by 8 or 9 field wires. The signal wires are grouped into 43 layers, and these layers are divided into 11 super-layers, with the labels SL- J (from the inside to the outside, $J = 1, 2, \dots, 11$). The SL-11 consists of only 3 signal layers, while each of the other 10 super-layers includes 4 signal layers. In some super-layers, the signal wires are parallel to the z axis of the MDC, so these super-layers are named axial super-layers. In the other super-layers, the signal wires have a stereo angle with respect to the z axis of the MDC, and these super-layers are named stereo super-layers. Axial (A) and stereo (U V, U means the stereo angle is negative, V means the stereo angle is positive) super-layers follow the order UVAAUUVUAA [3]. The small space around a signal wire and surrounded by the neighbouring field wires is called a drift cell. The sections of these drift cells are nearly square in the plane perpendicular to the beam axis, with the size of approximately 12×12 mm² in the innermost two super-layers and 16×16 mm² in the other super-layers. The signal wires collect the avalanche electrons produced by ionization along the particle trajectories. Electric signals on fired

Received February 7, 2022

* Supported by Ministry of Science and Technology of China (2009CB825200), Joint Funds of National Natural Science Foundation of China (11079008, 11121092), Natural Science Foundation of China (10905091) and SRF for ROCS of SEM.

1) E-mail: yuany@ihep.ac.cn

2) E-mail: xiaorui@gucas.ac.cn

3) E-mail: zhengyh@gucas.ac.cn

©2012 Chinese Physical Society and the Institute of High Energy Physics of the Chinese Academy of Sciences and the Institute of Modern Physics

wires are called hits and are used to reconstruct trajectories of charged particles.

One basic offline C++ software algorithm for MDC track reconstruction at BESIII is a pattern matching based tracking package (MdcPatRec) [4], which extracts track segments from a set of hits within a group of neighboring cells and links the segments into tracks. For charged particles with high transverse momentum (p_t), the tracking efficiency of MdcPatRec is satisfied for physics analysis. However, in low p_t range, the efficiency still has a large space to improve. In this paper we propose an extended segment construction scheme and its pattern dictionary which is justified to be helpful in the improvement of low p_t tracking efficiency.

2 MdcPatRec algorithm

To introduce the procedure of MdcPatRec, we list the important glossaries first:

(1) Segment. In a super-layer, a series of hits of a charged particle are defined as a segment. The arc in Fig. 1 shows a track. According to the segment definition, the 4 hits at the 4 fired wires compose a segment.

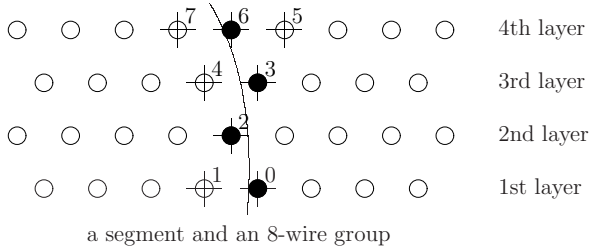


Fig. 1. A schematic plot for illustrating a segment and an 8-wire group. The 4 layers of circles denote the signal wires in one super-layer. The arc shows a track, and the black solid circles are the fired wires of the particle. The 8 adjacent signal wires marked with a cross compose an 8-wire group used to match the segment pattern in segment finding.

(2) Segment pattern and segment pattern dictionary. The fired wire distribution of a segment in a super-layer is defined as a segment pattern. In present MdcPatRec, segment finder uses the hits in the 2nd layer of a super-layer as seeds to search for segments in every group of 8 signal wires, the relative position of these signal wires is graphically represented by the 8 wires marked by a cross in Fig. 1. A segment pattern is expressed by 8 bits of an integer in C++ program: the fired wires are indicated by “1”, while the non-fired wires are indicated by “0”. For instance, the segment pattern illustrated in Fig. 1 is expressed with 01001101 in the binary number (77 in the decimal number). Segment patterns are collected to build a segment pattern dictionary.

The procedure of MdcPatRec includes the following steps: first to find segments in all super-layers by pattern matching; then to assemble segments in axial super-layers into circular tracks and apply a circle fit. Second, to add segments in stereo super-layers to circle tracks to constitute helix tracks and apply helix fit. After helix fit, tracks are reconstructed, and they are stored for Kalman fit, tracks extrapolation, physics analysis and so on.

3 The shortage of 8-wire segment pattern in MdcPatRec

The tracking efficiency of MdcPatRec is satisfied for non-curved tracks in the drift chamber. It loses some efficiency for low p_t tracks due to the reduced efficiency for segment finding within a super-layer. Azimuth coverage angle of segment groups does not meet the requirements for low p_t track segment finding.

Drift cell size limits the azimuth coverage of segment pattern dictionary. We compare the azimuth coverage of an 8-wire segment group with the azimuth coverage of tracks in a super-layer to test whether the segment group is large enough to reconstruct all possible segments. We define a variable $\Delta\phi$ to describe the coverage of a segment group along ϕ direction, the definition of $\Delta\phi$ is described by Eq. (1)

$$\Delta\phi = |\phi_{L-L(L-R)} - \phi_{U-R(U-L)}|, \quad (1)$$

where ϕ_{L-L} is the ϕ angle of the drift cell at the low left corner of an 8-wire group, as displayed in Fig. 1; similarly, $L-R$ means the low right corner, $U-L$ means the upper left corner, and $U-R$ means the upper right corner. The $\Delta\phi$ values of 8-wire segment pattern dictionary are listed in Table 1. We also define a variable, $\delta\phi$, to describe the azimuth coverage of a track in every super-layers along ϕ direction. In the magnetic field, $\delta\phi$ of a track with certain p_t within a super-layer can be calculated by Eq. (2).

$$\delta\phi = \left| \arctan\left(\frac{r_{in}^2}{\sqrt{4r_p^2 r_{in}^2 - r_{in}^4}}\right) - \arctan\left(\frac{r_{out}^2}{\sqrt{4r_p^2 r_{out}^2 - r_{out}^4}}\right) \right|. \quad (2)$$

In Eq. (2), r_{in} and r_{out} are the inner radius and outer radius of a super-layer respectively; r_p is the radius of a track with certain p_t , which can be calculated by Eq. (3)

$$r_p = \frac{p_t}{B_z \cdot q}, \quad (3)$$

where B_z is the magnetic field intensity along the beam axis and q is the electric charge of the particle; all variables are expressed in the international system of units.

The calculated $\delta\phi$ are listed in Table 2. Comparing these $\delta\phi$ with $\Delta\phi$ listed in Table 1, we find that the 8-wire segment pattern dictionary is not large enough to cover all segments of some low p_t charged particles.

The wire groups used to search for segments in the MDC are not all symmetric along ϕ direction. If the amounts of wires of two adjacent layers are the same, the two layers are staggered exactly by a half drift cell along ϕ direction, as shown in Fig. 1. Otherwise, the two layers cannot be placed in the exact staggered form. As a result, the symmetric arrangement of the wire groups in a super-layer is determined by the amounts of wires in the four layers. From SL-1 to SL-5, the amounts of wires in each layer are not the same, and some 8-wire wire groups in these super-layers are asymmetric. Figure 2 shows two asymmetric 8-wire wire groups in SL-1. As shown in these plots, the azimuth coverage of an asymmetric 8-wire wire group is smaller than that of a symmetric one. Table 1 lists the minimum wire group coverages of 8-wire seg-

ment pattern dictionary in every super-layer; as expected, the asymmetry of wire groups in SL-1 to SL-5 reduces the coverage of segment pattern. In addition, the 8-wire segment pattern dictionary is designed based on the hypothesis of symmetric wire groups, and the dictionary doesn't suit the asymmetric wire groups.

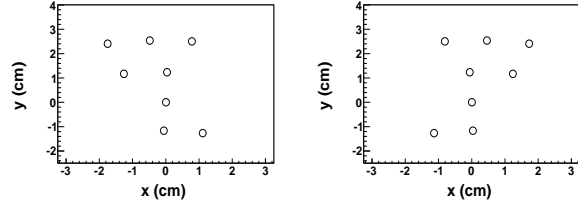


Fig. 2. The relative position of signal wires of 2 asymmetric 8-wire groups in SL-1. The origin of coordinate in each plot is set at the position of the signal wire in the second layer.

Table 1. The azimuth coverages, *i.e.* $\Delta\phi$ (degree), of 8-wire and 14-wire segment pattern dictionary in each super-layer.

The ‘min’ value is the minimum coverage in a super-layer. The wire groups are not all symmetric in SL-1 to SL-5, so the minimum $\Delta\phi$ is smaller than the symmetric wire groups. In SL-6 to SL-11, all wire groups are symmetric, so the minimum $\Delta\phi$ is equal to that of the symmetric wire groups.

Dictionary	SL-1	SL-2	SL-3	SL-4	SL-5	SL-6	SL-7	SL-8	SL-9	SL-10	SL-11
8-wire	18.6	12.4	10.9	8.4	6.7	5.6	5.1	4.3	3.8	3.5	2.5
8-wire min	10.9	7.9	6.8	5.2	4.1	—	—	—	—	—	—
14-wire	34.1	22.5	19.7	15.2	12.1	10.1	9.2	7.8	6.8	6.3	5.0
14-wire min	26.4	18.0	15.6	12.0	9.5	—	—	—	—	—	—

Table 2. The track azimuth coverage, *i.e.* $\delta\phi$ (degree), of charged particles with different p_t in every super-layer. If the p_t of a particle is smaller than 120 MeV/c, the particle curls in the MDC. If the $\delta\phi$ is larger than the minimum coverage of 8-wire segment pattern dictionary in this super-layer, it is marked with an underline. If the $\delta\phi$ is larger than the minimum coverage of 14-wire segment pattern dictionary in this super-layer, it is marked with an overline.

p_t (MeV/c)	SL-1	SL-2	SL-3	SL-4	SL-5	SL-6	SL-7	SL-8	SL-9	SL-10	SL-11
50	6.7	6.6	<u>11.2</u>	<u>16.9</u>							
70	4.7	4.5	6.8	<u>7.5</u>	<u>8.9</u>	<u>14.0</u>					
90	3.6	3.4	5.0	<u>5.3</u>	<u>5.6</u>	<u>6.4</u>	<u>8.0</u>	<u>11.9</u>			
110	2.9	2.8	4.0	4.1	<u>4.2</u>	4.5	<u>5.1</u>	<u>5.7</u>	<u>6.7</u>	<u>12.0</u>	
130	2.5	2.3	3.3	3.4	3.4	3.6	3.9	4.1	<u>4.4</u>	<u>5.4</u>	<u>4.1</u>
150	2.1	2.0	2.9	2.9	2.9	3.0	3.2	3.3	3.4	<u>3.9</u>	2.7
170	1.9	1.8	2.5	2.5	2.5	2.6	2.8	2.8	2.8	3.1	2.1

4 The extended segment pattern dictionary

In Sec. 3, we explain 8-wire segment pattern dictionary which is not optimal in the azimuth coverage for tracks with low p_t . In addition, the asymmetry of the wire groups aggravates this problem. Hence, it is meaningful to broaden the 8-wire groups to larger wire groups and design an extended segment pattern dictionary for segment

finding.

An easy way to broaden the coverage of the 8-wire segment pattern dictionary is to add a signal wire at each side of an 8-wire group on the 1st, the 3rd and the 4th layer, and an 8-wire group is extended to a 14-wire group as illustrated in Fig. 3. Comparing the azimuth coverage of particle tracks in Table 2 with the coverage of 14-wire segment pattern dictionary in Table 1, we can find that the

14-wire segment pattern dictionary can cover all segments of different tracks except the segments in the outermost super-layer, which a track can reach. This type of segments has very large azimuth coverage angle and cannot be reconstructed in an easy way.

A new segment pattern dictionary is built based on the 14-wire groups. Because the least squares fitting is applied to the hits of a segment pattern in segment finding, a segment pattern requires 3 or more hits. Therefore we build the dictionary with 3-hit and 4-hit segment patterns. A 4-hit segment pattern has a hit in every layer, and a 3-hit pattern has 3 hits in three different layers. For the 4-hit segment patterns, there are 80 ($4 \times 1 \times 4 \times 5$) combinations, but some combinations are obviously impossible and we remove them, which are determined by the relative position of the signal wires in a 14-wire group. From SL-6 to SL-11, all wire groups are symmetric, and we build a unique segment pattern dictionary for them. There is no significant asymmetry from SL-2 to SL-5 and we find that the dictionary based on symmetric wire groups is applicable. In SL-1, the asymmetry of wire groups is more serious than any other super-layers, and we build a special segment pattern dictionary. Finally the segment pattern dictionary for super-layers from SL-2 to SL-11 includes 30 4-hit segment patterns and 56 3-hit segment patterns, and the segment pattern dictionary for SL-1 includes 44 4-hit segment patterns and 72 3-hit segment patterns. Fig. 4 shows 6 4-hit segment patterns. In C++ program, a 14-wire segment pattern is expressed by 14 bits in an integer variable: the fired wires are marked by “1”, while the other

signal wires are marked by “0”. Table 3 lists the values of decimal numbers corresponding to the segment patterns drawn in Fig. 4.

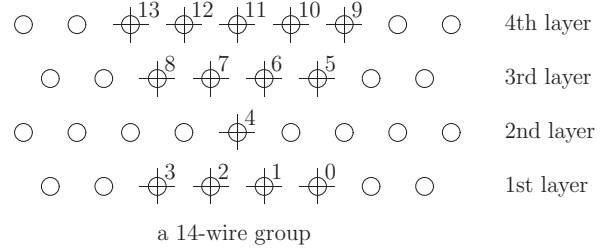


Fig. 3. A 14-wire group schematic plot. The 4 layers of circles denote the signal wires in a super-layer. The 14 adjacent signal wires marked with a cross make up the 14-wire group.

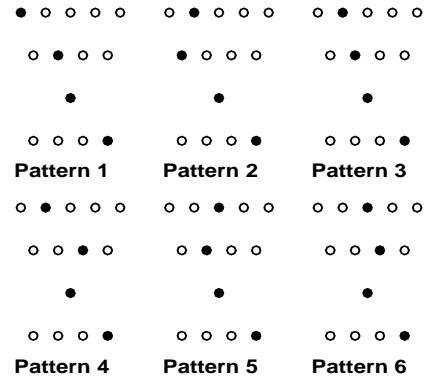


Fig. 4. Some 4-hit 14-wire segment patterns.

Table 3. The expression of the 4-hit segment patterns listed in Fig. 4.

pattern	decimal	binary	pattern	decimal	binary	pattern	decimal	binary
1	8337	10000010010001	2	4369	01000100010001	3	4241	01000010010001
4	4177	01000001010001	5	2193	00100010010001	6	2129	00100001010001

5 The 14-wire segment pattern dictionary performance

With single charged particle Monte-Carlo (MC) data sample, a multi-prong physics MC data sample and experimental data sample, the performance of 14-wire segment pattern dictionary is tested.

5.1 The segment efficiency

The segment efficiency ε_{seg} in a super-layer is defined as Eq. (4)

$$\varepsilon_{\text{seg}} = \frac{N_{\text{seg}}^{\text{rec}}}{N_{\text{seg}}^{\text{MC}}}, \quad (4)$$

where $N_{\text{seg}}^{\text{rec}}$ is the number of segments that have been found in a super-layer, and $N_{\text{seg}}^{\text{MC}}$ is the number of tracks passing through the super-layer in MC data sample. Figure 5 shows the segment efficiency of e^- with different p_t , as shown in these plots, the 14-wire segment pattern dictionary can achieve higher segment efficiency at the super-layer which track curled back.

5.2 The tracking efficiency

We generate 400,000 single e^- MC data sample to test the improvement of tracking efficiency. In the MC data sample, the momentum of e^- has a uniform distribution from 0.05 to 1 GeV/c, and the angular distribution of the e^- is uniform in full solid angle. Tracking efficiency ε_{trk}

is defined as Eq. (5)

$$\varepsilon_{\text{trk}} = \frac{N_{\text{trk}}^{\text{rec}}}{N_{\text{trk}}^{\text{MC}}}, \quad (5)$$

where $N_{\text{trk}}^{\text{rec}}$ is the number of events that have reconstructed a charged track, and $N_{\text{trk}}^{\text{MC}}$ is the number of events that have a charged track in MC data sample. Figure 6 shows the tracking efficiency for e^- . As shown in these plots, the tracking efficiency of 14-wire segment pattern dictionary is higher than that of the 8-wire segment pattern dictionary.

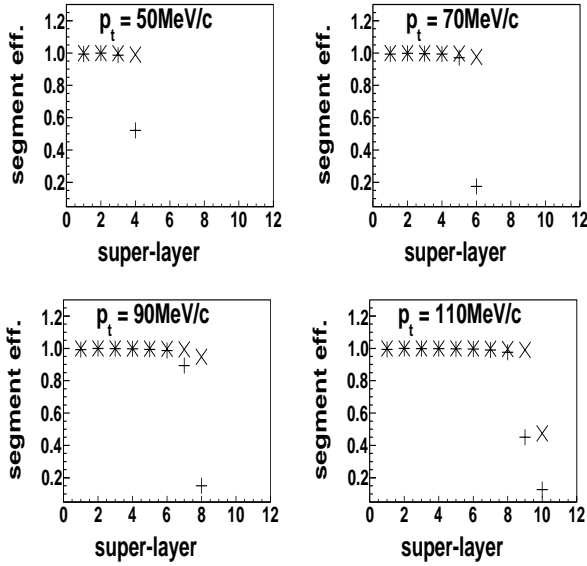


Fig. 5. The segment efficiency of e^- with different p_t in each super-layer. Symbol \times and $+$ are used to mark the segment efficiencies of 14-wire and 8-wire segment pattern dictionaries respectively.

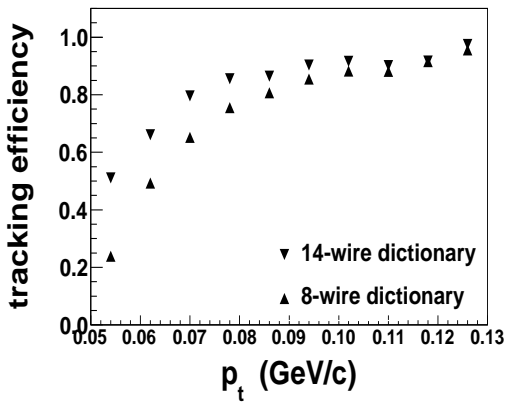


Fig. 6. The tracking efficiency of e^- .

5.3 The transverse momentum resolution

Using the same MC data sample we generate for testing the tracking efficiency, we compare the transverse momentum resolution between the extended pattern dictionary and the old pattern dictionary. The transverse momentum resolution δp_t is an index of track reconstruction quality. δp_t is expressed by Eq. (6)

$$\delta p_t = p_t^{\text{rec}} - p_t^{\text{MC}}, \quad (6)$$

where p_t^{rec} is the p_t of a reconstructed track, while p_t^{MC} is the p_t of this charged particle in MC simulation. Fig. 7 shows the δp_t distribution of e^- (p_t less than 130 MeV/c) reconstructed by the 14-wire and 8-wire segment pattern dictionaries respectively. By fit, the δp_t resolution is improved from about 0.94 MeV/c to about 0.89 MeV/c.

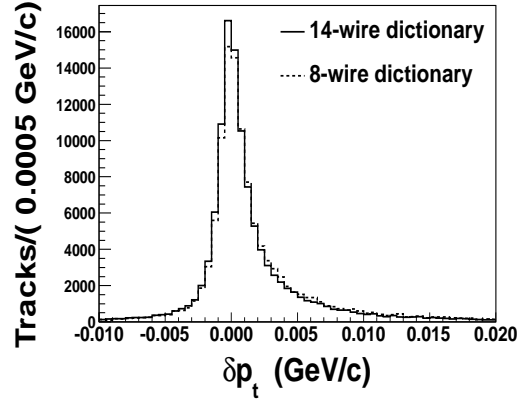


Fig. 7. The δp_t distribution of e^- . The two histograms are normalized.

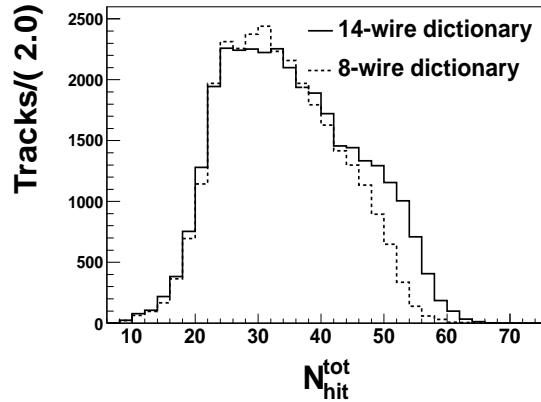


Fig. 8. The hits number distribution of e^- .

5.4 The noise resistant ability

With the same MC events that we use to test the tracking efficiency, we test the noise resistant ability of the extended pattern dictionary. The track hits number is the amount of hits used in the reconstructed tracks, and it determines the quality of track reconstruction. The track noise level R_{noise} can be used to denote the anti-noise

ability of tracking algorithm. The definition of R_{noise} is expressed by Eq.(7)

$$R_{\text{noise}} = \frac{N_{\text{hit}}^{\text{noise}}}{N_{\text{hit}}^{\text{tot}}}, \quad (7)$$

where $N_{\text{hit}}^{\text{noise}}$ is the number of fired wires used in track reconstruction but they are not fired by the particle; $N_{\text{hit}}^{\text{tot}}$ is the number of signal wires used in track reconstruction. Figure 8 and 9 display the number of hits on track and R_{noise} of e^- with p_t less than 130 MeV/c. In these plots, the average $N_{\text{hit}}^{\text{tot}}$ is increased from 33.1 to 34.9, while the average R_{noise} is decreased from 0.43% to 0.42%. The change of track noise level is very little.

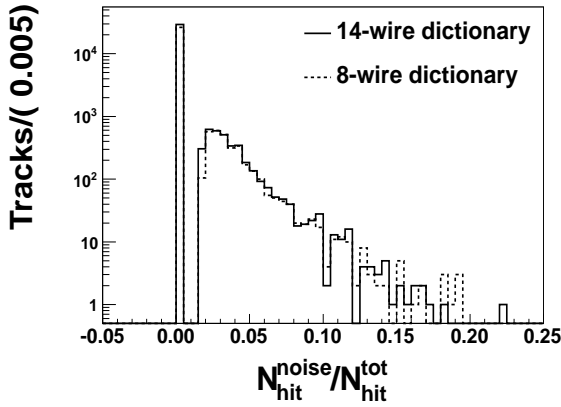


Fig. 9. The R_{noise} distribution of e^- .

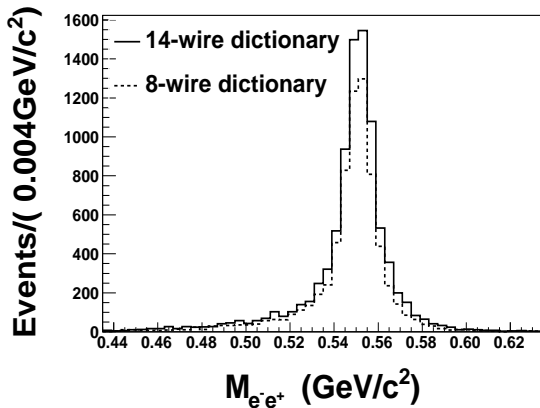


Fig. 10. The reconstructed signals of η from MC decay sample $\psi(2S) \rightarrow \gamma\chi_{cJ} \rightarrow \gamma\eta K^+ K^-$ with the requirement p_t of e^- less than 130 MeV/c.

5.5 Application in physics analysis

We generate a physics process, $\psi(2S) \rightarrow \gamma\chi_{cJ} \rightarrow \gamma K^+ K^- \eta \rightarrow \gamma K^+ K^- e^+ e^-$, to test the performance of the new segment pattern dictionary. Figure 10 is the invariant mass distribution of η . As shown in the plot, the

new segment pattern dictionary can keep more physical events than the old segment pattern dictionary. The total reconstruction efficiency is increased by about 4%; if we only count the events with p_t of e^- less than 130 MeV/c, the efficiency is increased by about 20%.

5.6 Application in experimental data

We test the new segment pattern dictionary with experimental data. Figure 11 shows the number of reconstructed tracks with respect to p_t for a sample of $\psi(3770)$ experimental data. The amount of reconstructed tracks with p_t less than 130 MeV/c is increased by about 15%. The number of charged tracks of a $\psi(3770)$ event is usually not less than 4. The differences in the number of charged tracks and in the track angular distribution between $\psi(3770)$ events and single e^- MC events make the difference between the curves of reconstructed tracks in Fig. 11 and efficiency curves in Fig. 6.

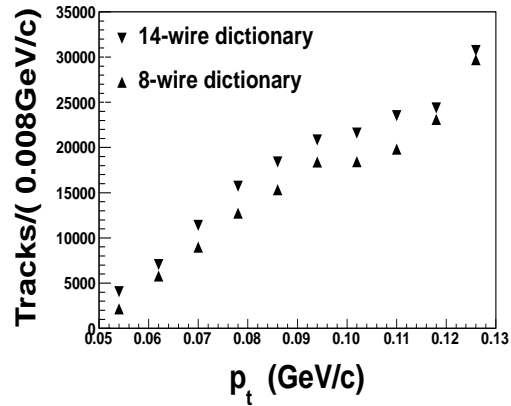


Fig. 11. The reconstructed tracks numbers from $\psi(3770)$ experimental data.

5.7 CPU-time consumption

Within BESIII offline software system [5], We test the CPU-time increase of MdcPatRec using the 14-wire segment pattern dictionary. Compared with using the 8-wire segment pattern dictionary, the CPU-time of MdcPatRec in segment finder is increased by about 2 ms for an event on the average; the CPU-time in total MdcPatRec algorithm is increased by about 30%; the CPU-time of the total event reconstruction is increased by about 10%.

6 Summary and discussion

In this paper, we study the issue of low tracking efficiency of the MdcPatRec algorithm in the low p_t range and understand one source of the problem as the shortage of 8-wire segment group: its limit of azimuth angle coverage and wire group asymmetry. We propose a 14-

wire group and its segment pattern dictionary as a remedy to the defect. The performance shows that the new wire group construction scheme and its segment pattern dictionary can improve the tracking efficiency for the low

p_t tracks. However, the CPU-time consumption is increased, so we will do more work to optimize the algorithm.

References

- 1 Ablikim M et al. (BESIII Collaboration), Nucl. Instrum. Meth. A, 2010, **614**: 345
- 2 CHAO K T et al. Modern physics A, 2009, **24** No.1 supp
- 3 Preliminary Design Report of the BESIII detector, Jan, (2004)
- 4 ZHANG Yao et al. HEP & NP, 2007, **31** (6):570 (in Chinese)
- 5 LI Weidong et al. The Offline Software for the BESIII Experiment, Proceeding of CHEP06, Mumbai, 2006